ELSEVIER

Contents lists available at ScienceDirect

Tribology International

journal homepage: www.elsevier.com/locate/triboint



Full Length Article

Transient Energy Released by a Tribological Process

Daniel Ingo Hefft (alp.)*, Megan J. Povey (blo),1, Zhenyu Jason Zhang (alp.)1

- a School of Chemical Engineering, University of Birmingham, Birmingham, B15 2TT, United Kingdom
- ^b School of Food Science and Nutrition, University of Leeds, Leeds, LS2 9JT, United Kingdom

ARTICLE INFO

Keywords: Transient energy Acoustic emission Tribology Tribo-acoustics Rheology Lubricants Ultrasound

ABSTRACT

This study investigates the relationship between transient energy releases and friction phenomena. We developed a theoretical framework to quantify frictional heating dynamics and transient energy dissipation at sliding interfaces, linking these processes to measurable acoustic emission (AE) waveforms. We identified three distinct AE regimes: (1) 300 kHz signals from micro-crack events, (2) 800 kHz asperity impacts with harmonic frequencies, and (3) broadband stick–slip chirps reflecting friction instabilities. For lubricated contacts, the model demonstrates how viscous damping alters energy release patterns. Key findings reveal that AE frequency content relates with interfacial mechanisms, namely subsurface fracture, elastic asperity collisions, and velocity-dependent friction transitions.

1. Introduction

Friction is a ubiquitous phenomenon that arises when two surfaces come into contact and move in a relative motion against each other [1], which is, in essence, a non-linear phenomenon [2]. The dissipation of energy through frictional processes is a crucial aspect of how these systems operate, as it converts kinetic energy mostly into heat. However, in certain situations, frictional processes can lead to a sudden release of energy, such as crack events [3] that are often associated with the formation and propagation of frictional instabilities [4], underpinning a variety of phenomena such as earthquakes and landslides.

One of the most common types of frictional instability is stick–slip motion, leading to the release of energy. The stick–slip motion is observed in a variety of situations [5], from the motion of a car on a road to the cleaning of a glass. The mechanisms that govern the initiation and propagation of stick–slip motion are complex. Recent advances in experimental techniques and computer simulations have provided some new insight into the underlying physics of these processes [6–10]. One possible explanation for the transient energy releases associated with the stick–slip motion is the sudden rupture of microscopic asperities on the surface in contact [8], which results in a rapid separation of the surfaces in contact and the release of the stored elastic energy. Another possible mechanism is the generation of waves or vibrations within the materials, leading to the release of energy in the form of acoustic emissions [11].

Understanding the dynamics of frictional processes and the transient energy released is therefore of significant scientific interest, as it has important implications for a range of fields, such as food processing [12],

seismology [13], hydrology [14,15], and engineering applications [16] whereby friction takes place at an interface. By developing a comprehensive understanding of the fundamental physics of the frictional processes, researchers may be able to establish the onset of frictional instabilities and develop strategies to mitigate their effects.

A significant effort in advancing this field was made by Woodhouse and his colleagues. Butlin and Woodhouse [17] investigated the complexities associated with experimentally validated low-order models for friction-induced vibration phenomena, which encompass a limited number of vibrational modes within each of the constituent sub-systems. One salient challenge lies in the increased sensitivity of friction-induced vibration systems to variations in parameters, which often results in difficulties in reproducing experimental outcomes, despite that the same model was deployed. The authors highlighted that the predictions of a low-order model could differ substantially from the assumed value of contact stiffness. Another challenge is to model the dynamics of a frictional process arising from the complexities of surface characteristics. Frictional force could fluctuate due to contact conditions, surface roughness, and sliding velocity [17]. The authors presented a systematic analysis of a system featuring two degrees of freedom, exploring its convergence behavior, while systematically varying the number of modes integrated into the model. Their model's predictions converge as additional modes are incorporated, although the rate of convergence is governed by the specific system of interest. The authors also investigated the sensitivity of these predictions to variations in contact parameters, and demonstrated that the contact

E-mail address: D.I.Hefft.1@bham.ac.uk (D.I. Hefft).

¹ Authors contributed equally.

^{*} Corresponding author.

Glossary		
Entry	Meaning	Description
A	Area	m^2
α	Thermal diffusivity	$m^2 s^{-1}$
β	Material constant	_
c_{p}	Specific heat capacity	$ m JK^{-1}kg^{-1}$
$\frac{c_p}{F_n}$	Normal force	N
h	Height	m
H	Hardness	_
k	Thermal conductivity	${ m W}{ m m}^{-1}{ m K}^{-1}$
μ	Coefficient of friction	_
P	Pressure	Pa
Q	Heat	J
ρ	Density	$kg m^{-3}$
S	Sliding distance	m
σ	Stress	$ m Nm^{-3}$
t	Time	S
u	Fluid velocity	$m s^{-1}$
v	Sliding velocity	$m s^{-1}$
V	Volume	m^3
x	Distance	m
η	Viscosity	Pa s
T	Absolute temperature	K

stiffness exerts the greatest influence on the accuracy of their predictions. Moreover, their assumed friction was another factor that could affect the accuracy of the prediction.

In a subsequent work [18], Butlin and Woodhouse presented a comprehensive investigation concerning the application of low-order mathematical models for the prediction of friction-induced vibration phenomena. The system under consideration comprises a disc and a pad interconnected via a sliding contact interface. A rigorous linear stability analysis of this system was developed, revealing its susceptibility to destabilization induced by frictional forces. A rigorous comparative analysis was carried out, wherein the model's predictions were compared with the results generated by an experimental apparatus. The results evidence that the model accurately predicted the frequencies and growth rates associated with the squealing instability phenomenon. Nevertheless, the model exhibits a sensitivity to the assumed parameter values, with particular emphasis on contact stiffness and dynamic friction. The specific work by Butlin and Woodhouse [18] is referenced in the present study for their friction-induced vibration model because firstly it offers a methodical exploration of the efficacy of low-order models for the prediction of specific forms of vibrational behavior. Secondly, it validates the model's capabilities to make prediction by affording a rigorous comparison between model predictions and experimental observations. Lastly, their work identifies the pivotal parameters exerting influence over the model's accuracy, thereby offering insights into the refinement of future models.

Nevertheless, there are certain limitations merit consideration. Primarily, the study by Butlin and Woodhouse [18] confines itself to a relatively simplistic system comprising a disc and a pad, prompting the question whether the model could be applicable in more intricate configurations. Secondly, the reliance on a linear stability analysis as the modeling foundation may not be universally applicable to all systems exhibiting friction-induced vibrations. Lastly, the model's susceptibility to variations in assumed parameter values poses practical challenges, which warrants future investigation and refinement.

A further advance made by Wang and Woodhouse [19] in understanding the dynamics of frictional processes and the associated transient energy released, in which a range of methodologies were employed in quantifying the frequency response of a dynamic friction. The authors described a novel experimental setup, comprising a pinon-disc tribometer augmented with an additional actuator to impart

a small sinusoidal perturbation to the sliding speed. The frictional force was measured by a loading cell, of which the results revealed a nuanced and non-monotonic frequency response, a characteristic prone to variation contingent upon material properties, sliding conditions, and the excitation frequency. The authors reported that the frequency response of the dynamic frictional force may exhibit negative values at certain frequencies. This counterintuitive behavior signifies that the friction force may intensify in response to the perturbations in sliding speed, which could be attributed to the nature of dynamic friction force, encompassing not only the dissipating components, but also those proportional to the sliding speed. Thus analysis of frictional forces must account for their amplitude and phase, and their time derivatives. The authors contend that the frequency response of a dynamic friction force constitutes an intrinsic attribute of sliding interfaces, thus clarifying the role of the dynamics underpinning friction-induced vibrations, such as brake squeal. However, certain limitations warrant consideration. Primarily, the experimental scope of the study limits to a selection of materials and sliding conditions, warranting future investigation to discern the generality of the observed frequency response patterns [20,21]. In addition, the absence of a theoretical framework explaining the observed frequency response presents an avenue for further exploration.

Woodhouse and co-authors explained the challenges associated with the development of dependable constitutive laws for dynamic friction [22]. They identified key challenges, including the non-linearity of the friction force with regards sliding velocity, normal load, and contact area, the influence of various factors such as surface roughness, temperature, and contaminants on friction force, and the inherent challenges in accurately measuring friction force, especially under dynamic conditions. The authors asserted that there is no universal constitutive law capable of accurately predicting friction across all conditions. However, they remained confident of the feasibility of establishing reliable constitutive laws that can approximate friction behavior.

Ultrasound is a powerful tool that has been used for decades to detect and diagnose material conditions [23–26]. However, in recent years, ultrasound technology has found a new application in the field of tribology, the study of friction, wear, and lubrication of surfaces in relative motion. Ultrasound can be used to monitor wear and friction by detecting changes in the acoustic emission (AE) generated by the friction and wear of materials. AE refers to the sound waves that are

generated by the motion of surfaces in contact with each other. When surfaces in contact experience friction and wear, they emit a range of frequencies that can be detected and analyzed using ultrasound sensors. By analyzing these signals, it is possible to identify the onset of wear and friction and track its progression over time. [27,28]

One key advantage of low-power ultrasound to monitor wear and friction is that it is a non-destructive evaluation technique that can be applied to a wide range of materials and surfaces [29]. Ultrasound sensors can be placed directly on the surface of a material, allowing for real-time monitoring of wear and friction without the need for disassembly or interruption of the system. This makes ultrasound monitoring an attractive option for applications where downtime is expensive or impractical, such as in industrial machinery or aerospace components.

Another advantage of ultrasound monitoring is that it is highly sensitive and can detect changes in wear and friction that may not be visible to the naked eye or other monitoring techniques. For example, ultrasound monitoring can detect the onset of wear in bearings or gears before they become visibly damaged, allowing for preventative maintenance to be performed before a catastrophic failure occurs. Ultrasound monitoring can also detect changes in friction that may be caused by changes in lubrication or other factors, allowing for adjustments to be made to optimize performance and extend the lifespan of components.

In addition, ultrasound monitoring can provide valuable insights into the nature of wear and friction in materials. By analyzing the frequency and amplitude of the acoustic emission signals [30], it is possible to determine the mechanisms of wear and friction, such as adhesion, abrasion, or fatigue. This information can be used to design better materials and lubricants that are more resistant to wear and friction, improving the performance and lifespan of components.

There are, however, some challenges associated with using ultrasound to monitor wear and friction events. The most obvious major challenge is the interpretation of the data generated by the sensors. The signals generated by the friction and wear events are usually complex and difficult to analyze, requiring specialized knowledge and expertise [31,32]. Additionally, the interpretation of the data can be affected by factors such as temperature, humidity, and other environmental conditions.

Another challenge is the development of suitable sensors and monitoring systems that can be deployed in a harsh manufacturing environment. Sensors may need to be designed to withstand operating conditions, such as high temperatures, high pressures, and exposure to chemicals and other corrosive substances. Additionally, monitoring systems may need to handle large amounts of data generated by the sensors and provide accurate and reliable analysis.

Despite these challenges, low-powered ultrasound monitoring is becoming an increasingly popular technique for monitoring wear and friction in a wide range of applications. Its non-invasive and non-destructive nature, high sensitivity, and ability to provide valuable insights into the nature of wear and friction make it an attractive option for industrial machinery, aerospace components, and other critical systems. As technology continues to evolve, it is likely that ultrasound monitoring will become even more widely used and sophisticated, allowing for better performance, greater efficiency, and increased reliability of systems and components.

To date, there is little understanding of the relationship between frictional phenomena and the associated acoustic characteristics despite its application in tribological studies [33,34]. The purpose of this work is to elucidate the fundamental relationship between transient energy released and frictional phenomena. We present models that address challenges such as the onset of a wear process. We also address pitting by cavitation as well as the effect of lubricants.

2. Fundamental definitions and relationships

2.1. Friction and stick-slip

Friction is the force that opposes the motion between two surfaces in contact. It arises from the interactions between the two surfaces and can be described by the Coefficient of Friction (CoF) that quantifies the amount of force required to overcome the frictional force and initiate motion. Stick-slip phenomenon arises from the interplay between the frictional force and the restoring force of the system. When two surfaces are in contact and are being moved relative to each other, the frictional force opposes the motion, while the restoring force tries to bring the surfaces back to their original position. When the applied force is small, the restoring force dominates and the surfaces remain in contact, resulting in stick. However, as the applied force increases, the frictional force also increases until it overcomes the restoring force, causing the surfaces to slip [35,36]. Stick-slip is a common phenomenon in many systems, including mechanical, geological, and biological systems [37-39] One of the challenges associated with the study of stick-slip is the complex nature of the phenomenon. Stick-slip events occur in a wide range of tribological conditions, and the behavior can be affected by a multitude of factors, including surface roughness, lubrication, temperature, and pressure. The stick-slip phenomenon can be characterized by several parameters, including the coefficient of friction, the amplitude and frequency of the motion, and the energy dissipated due to friction. These parameters can be used to model and predict the behavior of the system under different conditions and to design systems that exhibit specific stick-slip behavior. In summary, friction is the force that opposes motion between two surfaces in contact, and stick-slip is a specific type of friction characterized by a jerky, irregular motion of the surfaces as they move.

2.2. Transient energy release

Transient energy release refer to the sudden and brief energy releases that occur in various physical systems [15,40]. These energy releases are typically characterized by their short duration and high energy output. They can occur in a wide range of physical contexts, from astrophysical phenomena like supernovae and gamma-ray bursts to laboratory experiments involving high-energy particles. In many cases, transient energy releases are the result of sudden changes in the physical conditions of a system. These changes can lead to rapid release of stored energy in the form of radiation or kinetic energy. The principles of thermodynamics and statistical mechanics provide a framework for understanding the behavior of energy in complex physical systems. For example, thermodynamics describes the relationship between energy and temperature, while statistical mechanics describes how the behavior of individual particles contributes to the overall behavior of a system. An excellent example of research concerning transient energy releases is the study of plasma physics [41]. Transient energy releases can occur in plasma because of sudden changes in the plasma's magnetic or electric fields.

2.3. Ultrasound

Ultrasound is a form of transient energy release that is characterized by high-frequency, short wavelength (micrometers), and low amplitude [42]. These sound waves could be generated by a variety of sources, including mechanical vibrations, electrical discharges, and thermal energy. The range of frequencies used in ultrasound varies depending on the application. In medical imaging, for example, the frequencies used range from 2 to 18 MHz. In industrial testing, frequencies range from 20 kHz to 100 MHz. The wavelength is determined by the speed of sound in the medium through which the sound waves travels divided by the frequency and can range from several meters in air to a few micrometers in solids.

Ultrasound, as a technology, is deployed in a wide range of applications, including medical imaging [43], industrial testing [44,45], and materials science & chemistry [46,47]. For example, ultrasound is used to detect defects in materials, such as cracks or voids, and to measure the thickness of materials in industrial testing. In material science, ultrasound is used to study the properties of materials, such as their elasticity and strength as well as possibly engineering materials by controlling nucleation [48,49].

One type of energy release due to ultrasound is a process called acoustic cavitation. Transient acoustic cavitation occurs in fluids when high power high-frequency sound waves cause small bubbles or voids to form. When these bubbles collapse rapidly, they release a burst of energy in the form of fluid jets, heat, light, and sound. The energy released by acoustic cavitation is in general high, and it can be used for a variety of purposes, such as cleaning, welding, and cutting [42,50]. Bubbles produced by ultrasound may also oscillate in a stable manner, perhaps confusingly this is called 'stable cavitation' [51].

The energy released in ultrasound can also be used to generate heat [10], which is known as high-intensity focused ultrasound (HIFU), and it has a wide range of applications in medicine and industry [52]. In medicine, HIFU is used to treat a variety of medical conditions, including cancer, by targeting and destroying cancer cells with high-intensity sound waves. In industry, HIFU is used for welding and cutting, as well as for cleaning and sterilizing equipment. The amplitude of ultrasound used for industrial testing is typically low [53], meaning that the energy released is relatively low. However, the energy released in ultrasound can still be significant, particularly in high-intensity focused ultrasound applications.

In general, ultrasound cn be seen as a form of transient energy release produced by acoustic cavitation and crack propagation [12], which has been used for a variety of purposes, including medical imaging, industrial testing, and materials science. The frequency, wavelength, and amplitude of ultrasound are important parameters that determine the properties and applications of such form of energy. Crack propagation results in the release of powerful bursts of ultrasound due to the energy in the crack being dissipated in the form of acoustic waveforms.

3. Relationship between transient energy releases and friction

3.1. Assumptions

To develop a basic mathematical model that relates transient energy released with friction, one must take into account the physical processes involved in a tribological process, via which part of the mechanical energy is converted mostly into thermal energy due to the interfacial interactions between the two surfaces in contact [54,55]. For two flat surfaces in contact with each other and move relative to each other with a velocity of v, with a normal force F_n , the resulting Coefficient of Friction is μ . Both surfaces are initially at a temperature T_0 , and the frictional heating generates a transient temperature rise, ΔT , in the contact region.

The heat generated by the tribological process can be expressed as:

$$Q = \int_{0}^{t} \sigma v \Delta T \, dt \tag{1}$$

where σ is the stress in the contact region, which is given by:

$$\sigma = \frac{F_n}{A} \tag{2}$$

where A is the true area of contact between the surfaces. The transient temperature rise ΔT represents the time-dependent increase in temperature due to frictional heating. The transient temperature rise, denoted as ΔT , refers to the time-dependent increase in temperature at a specific point or region within a material due to frictional heating (or other energy dissipation processes). Unlike steady-state temperature, which assumes equilibrium between heat generation and

dissipation, the transient temperature rise accounts for the dynamic evolution of temperature over time before reaching steady-state conditions. It is governed by the heat conduction equation, incorporating material properties such as density ρ , specific heat capacity c_p , and thermal conductivity k, as well as the temporal and spatial variations in temperature, and can be described using the heat conduction equation:

$$\rho c_p \frac{\partial T}{\partial t} = k \frac{\partial^2 T}{\partial x^2} \tag{3}$$

where ρ is the density, c_p is the specific heat capacity, and k is the thermal conductivity of the surfaces in contact.

To solve this equation, one must specify the initial and boundary conditions. It is assumed that the surfaces are initially at a temperature T_0 , and that the temperature at the sliding interface is constant at $T_0 + \Delta T$ as the result of sliding. Another assumption to be made is that the temperature at a distance x from the sliding interface is constant at T_0 , resulting in the boundary conditions below:

$$T(x,0) = T_0$$

$$T(0,t) = T_0 + \Delta T$$

$$T(\infty,t) = T_0$$
 (4)

Using the separation of variables method, the temperature distribution exhibits both spatial and temporal dependence and can be expressed as:

$$T(x,t) = T_0 + \Delta T \left(1 - \operatorname{erf}\left(\frac{x}{2\sqrt{\alpha t}}\right) \right)$$
 (5)

where erf is the error function, and α is the thermal diffusivity, given by:

$$\alpha = \frac{k}{\rho c_p} \tag{6}$$

The transient energy release Q, which integrates the thermal response over space and time, is:

$$Q = \sigma v \int_0^t \Delta T \left(1 - \operatorname{erf} \left(\frac{x}{2\sqrt{\alpha t}} \right) \right) dx \tag{7}$$

3.2. Transient energy release and the coefficient of friction

The Coefficient of Friction μ is in its simplest form defined as the ratio of the tangential force F_t required to move a body along a surface to the normal force F_n pressing the body against the surface. This basic assumption, known as *Amontons'* law [55], will suffice to create initial models on this subject matter, however, the authors acknowledge that more advanced models such as *Johnson–Kendall–Roberts* [56] and *Derjaguin–Muller–Toporov* [57], which do reflect more accurately on real world applications. Using *Amontons'* law, the Coefficient of Friction μ is defined as:

$$\mu = F_t / F_n \tag{8}$$

The tangential force F_t is expressed as:

$$F_t = \sigma A_c \tag{9}$$

where σ is the shear strength of the material and A_c is the real contact area between the surfaces.

The transient energy release due to frictional heating can be expressed as:

$$Q_f(t) = \rho c_p A_c \int_0^t u^2(x, y, z, t') \sigma(x, y, z, T(x, y, z, t')), dx, dy, dz, dt'$$
 (10)

where ρ is the fluid density, c_p is the specific heat capacity, and u(x,y,z,t') is the velocity of the fluid at position (x,y,z) and time t'. The shear strength, $\sigma(x,y,z,T)$, is assumed to vary across the surface due to the local properties of the contacting surfaces and temperature T(x,y,z,t').

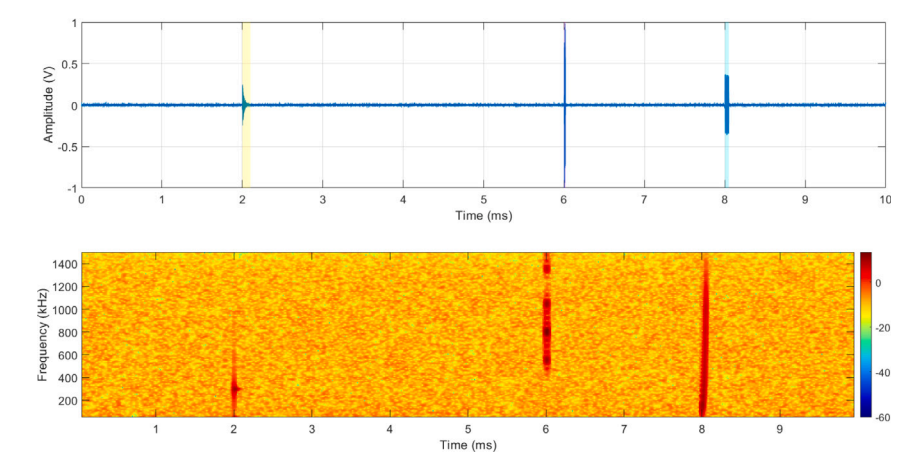


Fig. 1. Acoustic emission waveform in its time domain (top) and its time-frequency domain (bottom). Yellow highlight = Micro-crack event showing 300 kHz dominant frequency, purple highlight = Asperity impact with 800 kHz fundamental and 1.6 MHz harmonic, and light-blue highlight = Stick-slip chirp with time-frequency energy distribution.

The temperature distribution on the surface can be obtained from the heat conduction equation:

$$\nabla \cdot (k\nabla T) = \rho c_p \frac{\partial T}{\partial t} \tag{11}$$

where k is the thermal conductivity of the surface.

The real contact area A_c is related to the nominal contact area A_0 [58] and can be described by:

$$A_c = A_0 \exp\left(-\frac{H}{Q}\right) \tag{12}$$

where H is the hardness of the surface and Q is a material-specific constant.

The total energy release due to frictional heating over a period of time t can be obtained by integrating $O_f(t)$ over time:

$$E_f(t) = \int_0^t Q_f(t'), dt'$$
 (13)

The transient energy releases described in Sections 3.1 to 3.3 manifest as characteristic AE signals during tribological processes. Fig. 1 presents a multi-domain analysis of AE waveforms captured during sliding contact using an AMSY6 data acquisition system (Vallen Systeme, Germany) equipped with a VS900-F broadband sensor and linked via a AEP5 preamplifier (Vallen Systeme, Germany).

The acquired AE signal shows temporal localization of tribological events, with corresponding spectral features shown in Fig. 2.

The time-frequency decomposition reveals three distinct emission regimes corresponding to specific energy release mechanisms (Fig. 1):

- (i) Micro-crack events (yellow): Dominant at 300 kHz, these emissions correlate with subsurface crack propagation events where the energy release rate follows the temperature-dependent shear strength relationship. The lower frequency components suggest longer duration events, consistent with thermal diffusion timescales predicted by Eq. (7). The events align with the broadband previously reported by Baranov et al. [59] as well as work by Knak et al. [60].
- (ii) Asperity impacts (purple): The 800 kHz fundamental frequency and 1.6 MHz harmonic structure likely show elastic collisions between surface protrusions. The harmonic generation mechanism arises from nonlinear contact stiffness variations during impact unloading.
- (iii) Stick-slip chirps (light blue): The time-frequency spreading reflects the velocity-dependent friction transitions, where the instantaneous chirp frequency corresponds to the rate of interfacial shear stress development prior to slip rupture [61].

The AE signal processing workflow in MATLAB R2020B employed wavelet-based denoising and short-time Fourier transforms. This analytical approach directly informs the spatial–temporal integration of energy release $Q_f(t)$.

3.3. Considerations using lubricants

Consider two surfaces in contact, separated by a lubricant layer of thickness h, with a normal force of magnitude F_n acting between them. Let the surfaces have a coefficient of friction of μ , and let the surfaces slide relative to each other with a velocity of v. Assume that the surfaces and the lubricant are initially at a temperature T_0 , and that the frictional heating generates a transient temperature rise ΔT in the contact region.

Heat transfer in the lubricant layer using three-dimensional heat conduction can be described by:

$$\rho_l c_{pl} \frac{\partial T_l}{\partial t} = \nabla \cdot (k_l \nabla T_l) + Q_l \tag{14}$$

where ρ_l is the density, c_{pl} is the specific heat capacity, and k_l is the thermal conductivity of the lubricant. Q_l represents the heat generation due to viscous dissipation in the lubricant layer, which can be expressed as:

$$Q_I = \eta_a(|\nabla v|)^2 \tag{15}$$

where η_a is the apparent viscosity of the lubricant.

To describe the heat transfer in the solid surfaces the below applies:

$$\rho_s c_{ps} \frac{\partial T_s}{\partial t} = \nabla \cdot (k_s \nabla T_s) + Q_s \tag{16}$$

where ρ_s is the density, c_{ps} is the specific heat capacity, and k_s is the thermal conductivity of the solid surfaces. Q_s represents the heat generation due to frictional dissipation in the solid surfaces, which can be expressed as:

$$Q_{\rm s} = \sigma v(\mu - \mu_{\rm s}) \tag{17}$$

where μ_s is the steady-state friction coefficient between the two surfaces in the presence of the lubricant.

To obtain the pressure distribution in the lubricant layer, the Reynolds equation must be solved. The Reynolds equation takes into account the hydrodynamic pressure generated by the lubricant flow [62, 63]:

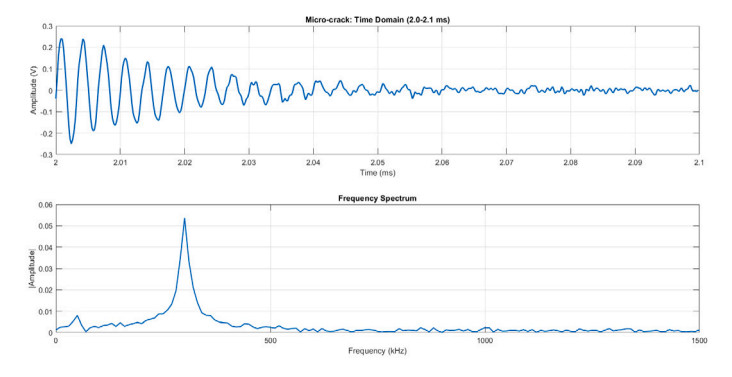
$$\nabla \cdot (h^3 \nabla P_l) = 12\eta h v \tag{18}$$

where h is the lubricant film thickness, and P_l is the pressure in the lubricant layer.

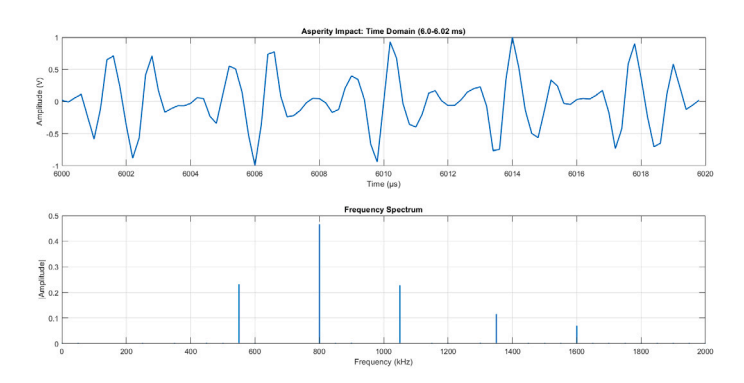
3.4. The coefficient of friction in the context of transient energy release

The coefficient of friction can be expressed as:

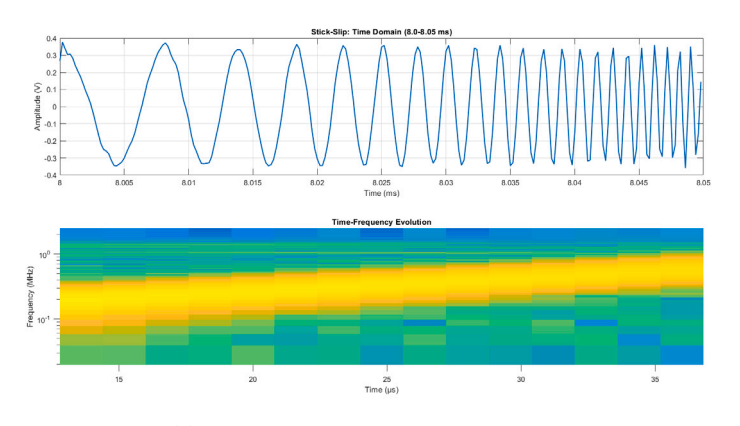
$$\mu = \mu_0 + \Delta\mu \tag{19}$$



(a) Detailed view of the micro-crack event.



(b) Detailed view of the asperity impact event.



(c) Detailed view of the stick-slip event.

Fig. 2. Detailed insights into events 3 a-c.

where μ_0 is the base friction coefficient between the two surfaces in the absence of the lubricant, and $\Delta\mu$ is the change in friction coefficient due to the presence of the lubricant. The change in friction coefficient $\Delta\mu$ can be expressed as:

$$\Delta\mu = \frac{\eta\gamma}{P_I/P_s} \tag{20}$$

where γ is the shear rate at the sliding interface, P_l is the pressure in the lubricant layer, and P_s is the pressure in the solid surfaces. The pressures P_l and P_s are obtained from solving the Reynolds equation for the lubricant layer.

The transient energy release Q is expressed as:

$$Q = \sigma v \int_0^t \int_A (\Delta T + \Delta T_l), dA$$
 (21)

where A is the contact area between the two surfaces, ΔT_l is the transient temperature rise in the lubricant layer, and the integral is taken over the contact area. The transient temperature rise in the lubricant layer ΔT_l can be obtained from the solution of the heat conduction equation for the lubricant layer, subject to appropriate initial and boundary conditions.

Conclusion

This work provides a unified framework to analyze transient energy releases in tribological systems, bridging theoretical models of frictional heating with experimental AE diagnostics. By solving the heat conduction equation under boundary conditions representing sliding interfaces, we derive the transient temperature distribution that quantifies how frictional energy localizes near the interface, with the

error function erf capturing the time-dependent penetration depth of thermal gradients. The integral formulation of transient energy release (Eq. (10)) further links shear stress σ , sliding velocity v, and contact area A to cumulative heat generation, providing a predictive tool for interfacial energy dissipation.

Experimental validation using AE transient recording (Fig. 1) provides us with three mechanistically distinct energy-release regimes. First, micro-crack nucleation events produce monopolar AE signals with a dominant frequency of 300 kHz (Fig. 2(a)), consistent with subsurface fracture dynamics in brittle surface layers. Second, asperity impacts generate high-frequency content at 800 kHz with 1.6 MHz harmonics (Fig. 2(b)), attributed to elastic rebound of deformed surface protrusions governed by Hertzian contact mechanics. Third, stick–slip instabilities exhibit broadband chirp-like AE signatures (50 to 600 kHz, Fig. 2(c)), reflecting system-scale velocity oscillations between static and kinetic friction states. These findings align with the model's prediction that energy release modes correlate with specific interfacial phenomena.

For lubricated contacts, the Reynolds equation (Eq. (18)) demonstrates that viscous dissipation in boundary layers alters pressure distributions and therefore suppresses high-frequency AE components. However, the model assumes constant lubricant properties and neglects non-Newtonian effects, limiting its accuracy for greases or polymer-containing lubricants.

However, this is an initial attempt to deliver a mathematical model aiming to link transient energy release phenomena to tribological events and limitations apply since this work makes use of some idealized assumptions: homogeneous contact pressure, temperature-independent material properties, and Gaussian surface roughness statistics.

For instance, the Reynolds equation (Eq. (18)) underestimates micro-elasto-hydrodynamic effects in nano-confined lubricants. Similarly, neglecting strain-rate dependence in shear strength σ would lead to over predicted energy release rates at sliding velocities where viscoplastic flow dominates. Addressing these limitations requires integrating stochastic contact models and high-strain-rate constitutive laws

Practically, this work enables two advances in tribological engineering:

- AE-based wear monitoring: The measured 300 kHz micro-crack signature (Fig. 2(a)) could provide an early warning indicator for subsurface fatigue, detectable prior to macroscopic wear scar formation.
- **Lubricant optimization**: By correlating the dimensionless pressure ratio P_l/P_s (Eqs. (14), (16)) with AE harmonic attenuation, lubricants can be formulated to suppress damaging asperity rebounds (event observed at 1.6 MHz).

Overall, this study establishes transient energy release as a useful technique for analyzing tribological systems. By unifying frictional heating models, lubricant rheology, and AE diagnostics, it provides a methodology to dissect interfacial energy dissipation mechanisms across scales. Future work will focus on strain-gradient plasticity extensions and synchrotron validations.

CRediT authorship contribution statement

Daniel Ingo Hefft: Writing – review & editing, Writing – original draft, Investigation, Conceptualization. Megan J. Povey: Writing – review & editing, Writing – original draft. Zhenyu Jason Zhang: Writing – review & editing, Writing – original draft.

Declaration of competing interest

The authors declare that the work described has not been published previously and that the article is not under consideration for publication elsewhere. The article's publication is approved by all authors. If accepted, the article will not be published elsewhere in the same form, in English or in any other language, including electronically without the written consent of the copyright-holder. The authors have no other relevant affiliations or financial conflict with the subject matters or materials discussed in the manuscript.

Acknowledgments

ZJZ and DIF wish to thank Dr John Williams, Emeritus Professor of Engineering Tribology of Robinson College (University of Cambridge), for sharing insights around advancements in the development of friction models. ZJZ would like to thank the EPSRC (EP/V029762/1) for the financial support.

Data availability

The data that has been used is confidential.

References

- [1] Suh NP, Sin H-C. The genesis of friction. Wear 1981;69:91-114. http://dx.doi. org/10.1016/0043-1648(81)90315-X.
- [2] Urbakh M, Klafter J, Gourdon D, Israelachvili J. The nonlinear nature of friction. Nat 2004;430(6999):525–8. http://dx.doi.org/10.1038/nature02750.
- [3] Yoshida S, Matsuoka J, Soga N. Evaluation of crack growth in glass by using stress-wave fractography. J Am Ceram Soc 1999;82(6):1621–3. http://dx.doi.org/ 10.1111/j.1151-2916.1999.tb01973.x.
- [4] Komijani M, Gracie R, Sarvaramini E. Simulation of induced acoustic emission in fractured porous media. Eng Fract Mech 2019;210:113–31. http://dx.doi.org/ 10.1016/j.engfracmech.2018.07.028.
- [5] Marton L, Lantos B. Modeling, identification, and compensation of stick-slip friction. IEEE Trans Ind Electron 2007;54:511–21. http://dx.doi.org/10.1109/ TIE.2006.888804.
- [6] Venkatadri TK, Henzel T, Cohen T. Torsion-induced stick-slip phenomena in the delamination of soft adhesives. Soft Matter 2023;19:2319–29. http://dx.doi.org/ 10.1039/D2SM01675C.
- [7] Ansari MA, Viswanathan K. Propagating Schallamach-type waves resemble interface cracks. Phys Rev E 2022;105:045002. http://dx.doi.org/10.1103/PhysRevE. 105.045002.
- [8] Yao W-W, Zhou X-P, Dias D, Jia Y, Li Y-J. Frictional contact and stick-slip: Mechanism and numerical technology. Int J Solids Struct 2023;274:112289. http://dx.doi.org/10.1016/j.ijsolstr.2023.112289.
- [9] Giordano S. Temperature dependent model for the quasi-static stick-slip process on a soft substrate. Soft Matter 2023;19:1813–33. http://dx.doi.org/10.1039/ D2SM01262F.
- [10] Baranov V, Kudryavtsev E, Sarychev G, Schavelin V. Friction of solids and nature of acoustic emission. In: Baranov V, Kudryavtsev E, Sarychev G, Schavelin V, editors. Acoustic emission in friction. 2007, p. 1–36. http://dx.doi.org/10.1016/ S0167-8922(07)80021-6, Chapter 1.
- [11] Kozochkin MP, Porvatov AN. Effect of adhesion bonds in friction contact on vibroacoustic signal and autooscillations. J Frict Wear 2014;35:389–95. http: //dx.doi.org/10.3103/S1068366614050080.
- [12] Varela P, Chen J, Fiszman S, Povey M. Crispness assessment of roasted almonds by an integrated approach to texture description: texture, acoustics, sensory and structure. J Chemom 2006;20(6–7):311–20. http://dx.doi.org/10.1002/cem.
- [13] Lockner D. The role of acoustic emission in the study of rock fracture. Int J Rock Mech Min Sci Geomech Abstr 1993;30:883–99. http://dx.doi.org/10.1016/0148-9062(93)90041-R
- [14] Baronti L, Castellani M, Hefft D, Alberini F. Neural network identification of water pipe blockage from smart embedded passive acoustic measurements. Can J Chem Eng 2022;100:521–39. http://dx.doi.org/10.1002/cjce.24202.
- [15] Hefft DI, Alberini F. A step towards the live identification of pipe obstructions with the use of passive acoustic emission and supervised machine learning. Biosyst Eng 2020;191:48-59. http://dx.doi.org/10.1016/j.biosystemseng.2019. 12.015
- [16] Wadley HNG, Scruby CB, Speake JH. Acoustic emission for physical examination of metals. Int Met Rev 1980;25(1):41–64. http://dx.doi.org/10.1179/imtr.1980. 25.1.41.

- [17] Butlin T, Woodhouse J. Friction-induced vibration: Should low-order models be believed? J Sound Vib 2009;328(1-2):92-108. http://dx.doi.org/10. 1016/j.jsv.2009.08.001, URL https://linkinghub.elsevier.com/retrieve/pii/ S0022460X90906269
- [18] Butlin T, Woodhouse J. Friction-induced vibration: Model development and comparison with large-scale experimental tests. J Sound Vib 2013;332(21):5302–21. http://dx.doi.org/10.1016/j.jsv.2013.04.045, URL https://linkinghub.elsevier.com/retrieve/pii/S0022460X13004021.
- [19] Wang S, Woodhouse J. The frequency response of dynamic friction: A new view of sliding interfaces. J Mech Phys Solids 2011;59(5):1020–36. http://dx.doi. org/10.1016/j.jmps.2011.02.005, URL https://linkinghub.elsevier.com/retrieve/ pii/S0022509611000330.
- [20] Palit Sagar S, Das S, Parida N, Bhattacharya DK. Non-linear ultrasonic technique to assess fatigue damage in structural steel. Scr Mater 2006;55(2):199–202. http: //dx.doi.org/10.1016/j.scriptamat.2006.03.037, URL https://www.sciencedirect. com/science/article/pii/S1359646206002387.
- [21] Giordano M, Calabro A, Esposito C, D'Amore A, Nicolais L. An acoustic-emission characterization of the failure modes in polymer-composite materials. Compos Sci Technol 1998;58(12):1923–8. http://dx.doi.org/10.1016/S0266-3538(98)00013-X, URL https://www.sciencedirect.com/science/article/pii/S026635389800013X.
- [22] Woodhouse J, Putelat T, McKay A. Are there reliable constitutive laws for dynamic friction? Philos Trans R Soc A: Math Phys Eng Sci 2015;373(2051):20140401. http://dx.doi.org/10.1098/rsta.2014.0401, URL https://royalsocietypublishing.org/doi/10.1098/rsta.2014.0401.
- [23] Adler L, Nagy P. Scanning acoustic microscopy for grain structure studies. In: MiCon 90: advances in video technology for microstructural control. 100 Barr Harbor Drive, PO Box C700, West Conshohocken, PA 19428-2959: ASTM International; p. 95–95–14. http://dx.doi.org/10.1520/STP17261S, URL http:// www.astm.org/doil.ink.cgi?STP17261S.
- [24] ASTM International. Standard practice for ultrasonic testing of wrought products. 2005, URL https://www.astm.org/Standards/E2375.htm.
- [25] ISO. Measurement and characterization of particles by acoustic methods Part 2: Linear theory. 2022, URL https://www.iso.org/standard/78454.html.
- [26] Worlton DC. Applications of lamb waves in ultrasonic testing. In: Symposium on nondestructive tests in the field of nuclear energy. 100 Barr Harbor Drive, PO Box C700, West Conshohocken, PA 19428-2959: ASTM International; p. 260–260–6. http://dx.doi.org/10.1520/STP42001S, URL http://www.astm.org/doil.ink.cgi?STP42001S.
- [27] Mujtaba M, Masjuki H, Kalam M, Ong HC, Gul M, Farooq M, Soudagar MEM, Ahmed W, Harith M, Yusoff M. Ultrasound-assisted process optimization and tribological characteristics of biodiesel from palm-sesame oil via response surface methodology and extreme learning machine - Cuckoo search. Renew Energy 2020;158:202–14. http://dx.doi.org/10.1016/j.renene.2020.05.158.
- [28] Du F, Hong J, Xu Y. An acoustic model for stiffness measurement of tribological interface using ultrasound. Tribol Int 2014;73:70–7. http://dx.doi.org/10.1016/ j.triboint.2013.11.015.
- [29] Dwyer-Joyce RS. The application of ultrasonic NDT techniques in tribology. Proc Inst Mech Eng Part J: J Eng Tribol 2005;219(5):347–66. http://dx.doi.org/10. 1243/135065005X9763.
- [30] Hase A, Mishina H, Wada M. Correlation between features of acoustic emission signals and mechanical wear mechanisms. Wear 2012;292–293:144–50. http: //dx.doi.org/10.1016/j.wear.2012.05.019.
- [31] Vallen H. AE testing fundamentals, equipment, applications. Non Destr Test 2002;7(9):1–24, URL https://www.ndt.net/article/v07n09/05/05.htm.
- [32] Baranov V, Kudryavtsev E, Sarychev G, Schavelin V. Simulation of characteristics of acoustic emission in friction. In: Baranov V, Kudryavtsev E, Sarychev G, Schavelin V, editors. Acoustic emission in friction. 2007, p. 37–96, Chapter 2.
- [33] Gutierrez R, Fang T, Mainwaring R, Reddyhoff T. Predicting the coefficient of friction in a sliding contact by applying machine learning to acoustic emission data. Frict 2024;12(6):1299–321. http://dx.doi.org/10.1007/s40544-023-0834-7, URL https://link.springer.com/10.1007/s40544-023-0834-7.
- [34] Brambilla L, Chalançon B, Roda Buch A, Cornet E, Rapp G, Mischler S. Acoustic emission techniques for the detection of simulated failures in historical vehicles engines. Eur Phys J Plus 2021;136(6):641. http://dx.doi.org/10.1140/epjp/s13360-021-01611-9, URL https://link.springer.com/10.1140/epjp/s13360-021-01611-9.
- [35] Overney RM, Takano H, Fujihira M, Paulus W, Ringsdorf H. Ansiotropy in friction and molecular stick-slip motion. Phys Rev Lett 1994;72:3546–9. http: //dx.doi.org/10.1103/PhysRevLett.72.3546.
- [36] Sokoloff J. The relationship between static and kinetic friction and atomic level "stick-slip" motion. Thin Solid Films 1991;206:208–12. http://dx.doi.org/10. 1016/0040-6090(91)90423-U.
- [37] Byerlee J. The mechanics of stick-slip. Tectonophys 1970;9:475–86. http://dx. doi.org/10.1016/0040-1951(70)90059-4.
- [38] Berman AD, Ducker WA, Israelachvili JN. Origin and characterization of different stick-slip friction mechanisms. Langmuir 1996;12:4559–63. http://dx.doi.org/10. 1021/la950896z.
- [39] Adams MJ, Briscoe BJ, Johnson SA. Friction and lubrication of human skin. Tribol Lett 2007;26(3):239–53. http://dx.doi.org/10.1007/s11249-007-9206-0.

- [40] Boyd JW, Varley J. The uses of passive measurement of acoustic emissions from chemical engineering processes. Chem Eng Sci 2001;56:1749–67. http://dx.doi.org/10.1016/S0009-2509(00)00540-6.
- [41] Rao YK, Srivastava AK, Kayshap P, Wilhelm K, Dwivedi BN. Plasma flows in the cool loop systems. Astrophys J 2019;874:56. http://dx.doi.org/10.3847/1538-4357/ab0665
- [42] Povey M. Ultrasonic techniques for fluids characterization. San Diego: Elsevier; 1997, http://dx.doi.org/10.1016/B978-0-12-563730-5.X5000-4.
- [43] Doi K. Diagnostic imaging over the last 50 years: research and development in medical imaging science and technology. Phys Med Biol 2006;51(13):R5–27. http://dx.doi.org/10.1088/0031-9155/51/13/R02.
- [44] Mason TJ, Riera E, Vercet A, Lopez-Buesa P. Application of ultrasound. In: Emerging technologies for food processing. Elsevier; 2005, p. 323–51. http://dx.doi.org/10.1016/B978-012676757-5/50015-3.
- [45] Metilli L, Morris L, Lazidis A, Marty-Terrade S, Holmes M, Povey M, Simone E. Real-time monitoring of fat crystallization using pulsed acoustic spectroscopy and supervised machine learning. J Food Eng 2022;335:111192. http://dx.doi. org/10.1016/j.jfoodeng.2022.111192.
- [46] Suslick KS, Price GJ. Applications of ultrasound to materials chemistry. Annu Rev Mater Sci 1999;29(1):295–326. http://dx.doi.org/10.1146/annurev.matsci. 29.1.295.
- [47] Cobley A, Mason TJ, Paniwnyk L, Saez V. Aspects of ultrasound and materials science. In: Chen D, Sharma SK, Mudhoo A, editors. Handbook on applications of ultrasound. Boca Raton: CRC Press; 2011, p. 63–96. http://dx.doi.org/10.1201/ b11012-9, Chapter 3.
- [48] Povey MJ, Ettelaie R, Lewtas K, Price A, Lai X, Sheng F. "Sounding" out crystal nuclei—A mathematical-physical and experimental investigation. J Chem Phys 2023;158(17). http://dx.doi.org/10.1063/5.0139811.
- [49] Povey MJ. Crystal nucleation in food colloids. Food Hydrocolloids 2014;42:118–29. http://dx.doi.org/10.1016/j.foodhyd.2014.01.016.
- [50] Ashokkumar M. The characterization of acoustic cavitation bubbles An overview. Ultrason Sonochemistry 2011;18(4):864–72. http://dx.doi.org/10. 1016/j.ultsonch.2010.11.016.
- [51] Leighton TG. The acoustic bubble. London: Elsevier; 1994, http://dx.doi.org/10.1016/B978-0-12-441920-9.X5001-9, URL https://linkinghub.elsevier.com/retrieve/pii/B9780124419209X50019.
- [52] ter Haar G, Coussios C. High intensity focused ultrasound: Physical principles and devices. Int J Hyperth 2007;23(2):89–104. http://dx.doi.org/10.1080/02656730601186138.
- [53] Parsons JE, Cain CA, Fowlkes JB. Cost-effective assembly of a basic fiber-optic hydrophone for measurement of high-amplitude therapeutic ultrasound fields. J Acoust Soc Am 2006;119(3):1432–40. http://dx.doi.org/10.1121/1.2166708.
- [54] Stieß M. Mechanische verfahrenstechnik partikeltechnologie 1. 3rd ed.. Springer-lehrbuch, Berlin, Heidelberg: Springer Berlin Heidelberg; 2009, http://dx.doi.org/10.1007/978/3-540-32552-9.
- [55] Israelachvili JN. Friction and lubrication forces. In: Intermolecular and surface forces. 3rd ed.. Burlington: Elsevier; 2011, p. 469–99. http://dx.doi.org/10.1016/ B978-0-12-375182-9.10018-1, Chapter 18 -Frict.
- [56] Borodich FM. The Hertz-type and adhesive contact problems for depth-sensing indentation. In: Bordas SPA, editor. Advances in applied mechanics. Volume 47. London: Academic Press/Elsevier; 2014, p. 225–366. http://dx.doi.org/10.1016/ B978-0-12-800130-1.00003-5, URL https://linkinghub.elsevier.com/retrieve/pii/ B9780128001301000035.
- [57] Violano G, Afferrante L. On DMT methods to calculate adhesion in rough contacts. Tribol Int 2019;130:36–42. http://dx.doi.org/10.1016/j.triboint.2018. 09.004, URL https://linkinghub.elsevier.com/retrieve/pii/S0301679X18304444.
- [58] Lyashenko IA, Pastewka L, Persson BNJ. On the validity of the method of reduction of dimensionality: Area of contact, average interfacial separation and contact stiffness. Tribol Lett 2013;52(2):223–9. http://dx.doi.org/10.1007/ s11249-013-0208-9, URL http://link.springer.com/10.1007/s11249-013-0208-9.
- [59] Baranov V, Kudryavtsev E, Sarychev G, Schavelin V. Friction of solids and nature of acoustic emission. In: Briscoe BJ, editor. Acoustic emission in friction. 1st ed.. Moscow: Moscow State Engineering Physics Institute/ Elsevier; 2007, p. 16.
- [60] Knak M, Wojtczak E, Rucka M. Crack monitoring in concrete beams under bending using ultrasonic waves and coda wave interferometry: the effect of excitation frequency on coda. J Phys: Conf Ser 2024;2647(18):182004. http: //dx.doi.org/10.1088/1742-6596/2647/18/182004, URL https://iopscience.iop. org/article/10.1088/1742-6596/2647/18/182004.
- [61] Wei J, Fatikow S, Li H, Zhang X. Design and waveform assessment of a flexible-structure-based inertia-drive motor. Micromachines 2019;10(11):771. http://dx.doi.org/10.3390/mi10110771, URL https://www.mdpi.com/2072-666X/10/11/771
- [62] Shukla J, Kumar S, Chandra P. Generalized reynolds equation with slip at bearing surfaces: Multiple-layer lubrication theory. Wear 1980;60(2):253–68. http://dx.doi.org/10.1016/0043-1648(80)90226-4.
- [63] Bayada G, Chambat M. The transition between the Stokes equations and the Reynolds equation: A mathematical proof. Appl Math Optim 1986;(1):73–93. http://dx.doi.org/10.1007/BF01442229.